GRAPHITE ATOMIC REFLECTION PLANE SPACING FROM THE DIFFRACTION OF ELECTRONS OF VARIOUS ENERGIES

A PREPRINT

Nathan C. Pierce

Department of Physics (Undergraduate)

University of Michigan - Dearborn

4901 Evergreen Rd, Dearborn, MI 48128

piercen@umich.edu

April 14, 2021

ABSTRACT

The distance between atomic reflection planes (d_{11} and d_{10}) resulting in two distinct diffraction maxima are determined by collecting data for the diffraction of various electron wavelengths through a polycrystalline graphite sample. Different incident electron wavelengths were produced by means of a $5\,\mathrm{kV}$ power supply. Using a diffraction tube, the diameters of two distinct diffraction maxima were measured over five trials. The planar spacings are deduced by application of Bragg's Law using two different methods. Method 1 calculates an average value using Bragg's Law: $\overline{d_{11}} = 2.4 \pm 0.1$ and $\overline{d_{10}} = 1.31 \pm 0.05$. Method two uses the slope of best fit from a diameter vs. inverse-square voltage plot: $d_{11} = 2.8 \pm 0.3$ $d_{10} = 1.33 \pm 0.12$.

1 Introduction

Thomas Young's double slit experiment, performed in 1801, is famous for demonstrating the wave-particle duality of light. Later, Louis de Broglie would propose the the wave-particle nature of matter. Experiments at Bell Laboratories by Clinton Davvison and Lester Germer [1] would

[1] Krane, "Modern Physics"

be the first evidence which supported de Broglie's claim. In their experiment, a beam of electrons is produced by a heated filament, which is then passed through a sample of nickle, resulting in diffraction patterns. Diffraction and interference are both unique properties of waves.

This experiment uses a similar setup. One key difference is that graphite serves as the sample. Voltage supplied to a heated cathode in a diffraction tube serves as the experimental control. Diffraction maxima appear in the form of two rings on a fluorescent screen. By varying the voltage, electrons of different wavelengths are produced, and the diffraction maxima are changed.

Such an experiment serves two primary purposes: confirmation of the wave-particle duality of matter, and understanding of the atomic structure of whatever solid state that serves as the diffraction grating. Different properties of the diffraction pattern reveal much information, such as the type of crystal structure of the sample, and the distances between the atomic planes of reflection within the crystal lattice.

Graphite produces two visible diffraction maxima in the shape of rings, indicating a polycrystalline structure. By measuring the radii of the diffraction rings over various voltages, the reflection plane distances can be determined. The primary focus of this experiment is determining this distance. The very appearance of wave interference in the form of the ring maxima is indicative of the validity of de Broglie's hypothesis.

This paper is broken up in to four sections. In order, they are theory, methods, results & discussion, and finally the conclusion.

2 Theory

Louis de Broglie's prediction is encapsulated by the equation:

$$\lambda = \frac{h}{p} \tag{1}$$

Observations of interference patterns are among the most compelling evidence of wave nature. Historically, the wave nature of particles have been probed by double-slit experiments, where particles are beamed through optical grating.

Using the regular spacing between atoms in a crystal as a substitute for man-made optical grating was first used in the experiments of Laue and Bragg. Electrons reflected from crystal lattices strike a detector and form diffraction patterns. The diffraction maxima for electrons are given by the Bragg equation:

$$2dsin(\theta) = n\lambda \tag{2}$$

Where n is a positive integer. The $2d$ factor comes from the extra distance that a beam of reflected electrons must travel for planes separated a distance d, compared to the beam that is deflected at the 'first' reflection plane. The angle θ is the angle of incidence for the electron beam (with respect to the reflection plane). Figure 2 shows a diagram

of this situation. The equation says that diffraction maxima (constructive interference) will only occur when the path difference for two beams is equal to integral numbers of the wavelength of the particle.

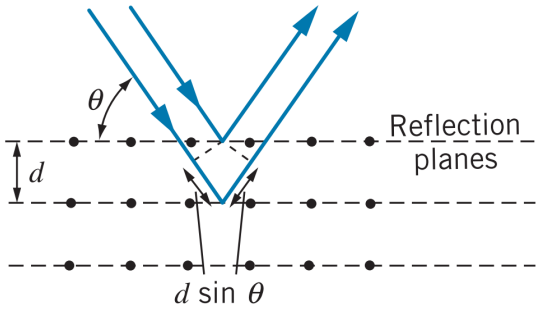

Figure 1. Diffraction of beams (blue lines) through a crystal lattice. The dots represent lattice points. The bottom beam travels an extra distance $2dsin(\theta)$ relative to the top beam. The dots are lattice points of the crystal structure. Note that the reflection plane was arbitrarily chosen - there is no basis for selecting the reflection planes. Source: "Modern Physics", Krane

The distance between lattice points in the crystal structure of graphite is $|\hat{a_1}| = 2.46\,\text{Å}$. One other important result from the geometry of hexagonal structure is that the ratio of plane spacings resulting in the two observable diffraction maxima $\frac{d_{11}}{d_{10}}$ is $\sqrt{3}$.

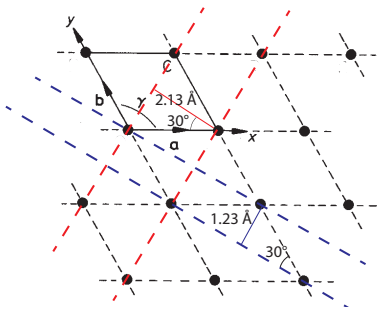

Figure 2. The distance between each lattice point is $a = b = 2.46\,\text{Å}$, and angle $\gamma = 120^\circ$ for the graphite crystal structure used in the experiment. The solid blue line represents the distance between reflection planes resulting in the inner ring, $d_{10} = 1.23\,\text{Å}$, and the red line represents the distance between reflections planes resulting in the outer ring, $d_{11} = 2.13\,\text{Å}$

The diffraction pattern shape depends primarily on the polycrystalline structure of the sample. The crystal structure of any solid is defined by the sum of two quantities: a lattice and a basis. To construct the crystal structure, the lattice must be determined, then the basis can be added to every point. The crystal structure of graphite is created from a two-dimensional hexagonal lattice (called graphene), where each carbon atom is bonded to two other carbon atoms. This forms the basis of graphite[2].

There are three material types of interest when considering the diffraction patterns[3]: single crystals, polycrystals, and amorphous materials. The graphite sample used here is polycrystalline. When an electron beam passes through such a material, the pattern are rings which are produced by the net effect of the beam passing through many orientations of crystals in the polycrystal lattice. There are an infinite number of reflection planes within a lattice.

[2]Dodd, et al. "Crystal Structure of Graphite, Graphene and Silicon"

[3]Welch Scientific Co. "Electron Diffraction Tube"

Each electron in the diffraction beam is subject to some potential difference which accelerates the particle to non-relativistic speeds, in the process acquiring kinetic energy $K = e\Delta V$, where e is the charge of the electron and ΔV is the potential difference, and thus a momentum:

$$p = \sqrt{2m_e K} \tag{3}$$

Using the de Broglie wavelength, the wavelength of the electrons are:

$$\lambda = \sqrt{\frac{h^2}{2m_e eV}} \tag{4}$$

Which can be reduced to a single constant term:

$$\lambda(\text{Å}) = \sqrt{\frac{150}{V}} \tag{5}$$

Note that the wavelength of the electrons depends on the potential.

Using this equation and Bragg's Law (Eq 2), it can be shown that the radius of each diffraction ring is proportional to the voltage:

$$D = \frac{2L}{d}\sqrt{\frac{150}{V}} \tag{6}$$

Where D is the diameter of the diffraction ring, L is the distance from the sample to the detector, and d is the length between atomic planes for each unique maxima. From this equation, it should be expected that the radius of each maximua should shrink with increasing voltage. Eq 6 allows the direct tabulation of d - by measuring D as a function of V.

The number of detectable maxima is related to the number of reflection planes which produce the largest d. Since there are an infinite number of orientations of reflection planes in the lattice, there are an infinite number of possible diffraction patterns (constrained by the crystal structure itself), but only the largest few d which satisfy Bragg's equation (Eq 2) will result in a noticeable intensity on the detector.

3 Methods

The apparatus used in the experiment was the TEL555 diffraction tube. The primary power supply was the TEL Atomic 5kV power supply. In addition to this, an HP Power Supply was also used. To monitor current to the anode, a Fluke 115 RMS DMM was used. See Fig 4 for a photograph of the setup. Refer to Fig 3 for a line diagram of the experimental setup.

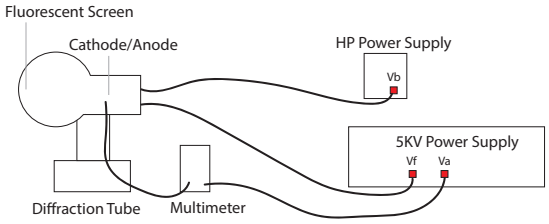

Figure 3. The apparatus used in the experiment.

The TEL 555 diffraction tube consists of a gun which emits a converging electron beam through an evacuated transparent glass bulb on to a luminescent screen (the tube is evacuated to prevent collisions between the electrons and gas molecules). The cathode ray passes through the graphite sample which is supported in the tube via a fine mesh-grid. The filament (serving as the cathode ray source) is an indirectly-heated oxide-coated cathode. Electrical connections to the filament are made via a $4\,\mathrm{mm}$ plug in the back of the apparatus and similarly for the anode with a connection on the side of the tube. Nominal anode voltage is given between $3.5\,\mathrm{kV}$ - $5\,\mathrm{kV}$ (see Fig 5 for the circuit diagram).

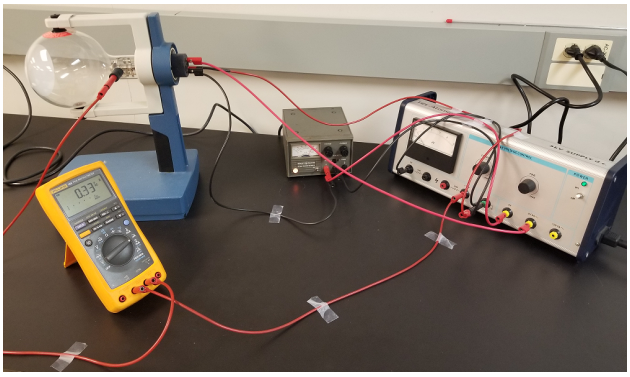

Figure 4. The experimental setup. Note the cable management to prevent crossing of the high potential output of the 5kV supply (right) with a lower potential.

Due to the high voltage necessary in the experiment, some safety precautions were taken. The Fluke DMM was used to monitor current supplied to the anode of the diffraction tube - exceeding $200\,\mu\mathrm{A}$ could damage the graphite sample, so care was used to monitor the current while adjusting the voltage on both of the power supplies throughout the experiment. Care was also taken to prevent damaging the glass diffraction tube, which was under vacuum. Additionally, there was some inherit risk while dealing with the 5kV power supply - to minimize risk, extra cable management was used to prevent the crossing of any high-potential wires with low-potential. Such crossing could result in an arc flash. Tape was used to keep the cabling secure and tidy. While the high-voltage power supply was on, extra precaution was taken to avoid touching any of the high-voltage lines.

The electrical components of the experimental setup were wired according to the diagram in Fig 5. The connection that ran directly from the high-voltage terminal of the TEL555 Power Supply was broken with an ammeter to keep track of the current supplied to the anode. As noted, there were two power supplies used in the experiment which supplied three different voltages: the voltage for the anode (high-voltage) V_A (for anode) and the small HP power supply V_B. The third voltage came from the constant 6V power supply on the TEL555. This voltage is denoted V_F, and it supplied power for the filament.

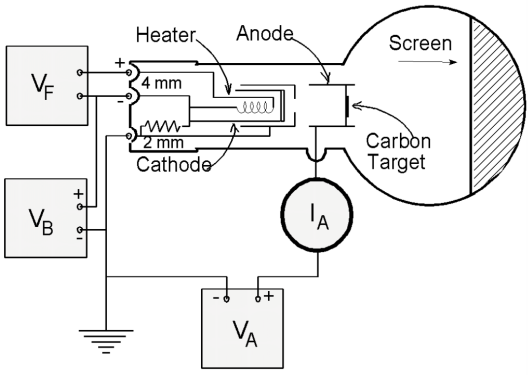

Figure 5. Source: webphysics.davidson.edu

Before providing a voltage to the anode, the filament was powered on via the 6 V supply. A period of about 1 minute was given to allow for the filament to warm up before V_A was adjusted. After this period, the voltage to the anode was slowly dialed up from the minimum voltage to about 2.5 kV.

Five sets of data were collected over a voltage range 2.5 kV - 4.9 kV, over intervals of 0.2 kV. For every voltage V_A, both the diffraction maxima radius of the inner and outer rings were measured. A Chicago-brand vernier-scale caliper was used to measure the radius ($\delta R = 0.002\,\mathrm{cm}$). To keep consistency in the measurements for all trials, the radius of each diffraction ring is defined and was measured as such: the distance from the inner edge of the diffraction ring (the rings were of some significant thickness) to roughly the middle of the central dot on the screen.

For four of the data sets, the measurements were made sequentially from a low to high voltage. One set of data was collected in which the voltage was selected 'at random' (where it was sufficiently random to peak a non-sequential voltage from the list by whim). This is trial 2.

Two different methods were used to test the Bragg diffraction theory (Eq 2) with the data from each of the 5 trials. Python routines in the Numpy, SciPy and Pandas libraries were used in both. The first method used Bragg's Law of Diffraction (2) to solve for d. The wavelength which appears in this equation was tabulated from Eq 5. The angle θ was calculated using the relations $tan(2\theta) = \frac{R}{L}$, where R are the two different radii and L is the length from the sample to the screen (13.5 cm). This process was carried out for both the inner R_{in} and outer R_{out} radii, at each voltage. To determine d_{11} (inner ring atomic plane spacing) and d_{10} (outer ring), the sum of all d_n for a given trial were divided by the number of data points (12 samples for every trial) to give the average value.

The second method used the slope of best fit for the data collected for each trial, using the relation in Eq 6. The slope of this plot m is linear, and must be equivalent to $\frac{2L}{d}\sqrt{150}$ by the same equation. d can be solved for, and since all other parameters are known, d can be determined. Best fit parameters were generated for the data in each trial.

4 Results and Discussion

The two Bragg diffraction rings became visible at 2.5 kV, confirming the polycrystalline structure of the graphite sample. Adjusting the voltage (and therefore also the wavelength of the electrons, by Eq 5) clearly results in a change in the diameter of the diffraction maxima, just as Eq 6 predicts.

Two issues were encountered related to measurement of the diffraction ring radii. The first: for lower anode potentials V_A, the rings had a diffuse, 'fuzzy' appearance. This made determining the inner edge of each diffraction ring, as well as the approximate center of the central dot on the screen, a challenge. This issue could be offset some-

what by adjusting V_B to increase the current to the anode (thereby increasing brightness of the diffraction maxima), but this process only mitigated the problem slightly because the rings were still 'fuzzy' or 'diffuse'. The readings taken at the higher anode voltages (near the $4.9\,\mathrm{kV}$ range) were much easier to take as the diffraction peak rings had a much less diffuse appearance and had more defined edges, making measurements easy.

The second issue: the geometry of the screen. The screen adhered to the spherical surface of the diffraction tube, meaning that the radii were measured on a sphere. This resulted in some difficulty in ensuring that the caliper was at two right angles to the point of contact on the spherical diffraction tube where the readings occurred (if the caliper was at some other angle, measurement would be slightly skewed). These two issues likely contribute to the random error associated with measurement of the radii of the diffraction peaks.

4.1 Method 1: Average Plane Spacing

The average atomic reflection plane spacings for the inner and outer diffraction rings ($\overline{d_{11}}$ and $\overline{d_{10}}$, respectively) are given in Table I. These are compared against the theoretical values of $d_{11} = 2.13$ Å (inner ring) and $d_{10} = 1.23$ Å (outer ring) (see Fig 2).

Trial	$\overline{d_{11}}$ (Å)	$\delta_{d_{11}}$ (%)	$\overline{d_{10}}$ (Å)	$\delta_{d_{10}}$ (%)
1	2.287 ± 0.019	7.38	1.272 ± 0.009	3.45
2	2.4 ± 0.1	10.49	1.31 ± 0.05	6.25
3	2.29 ± 0.02	7.67	1.305 ± 0.009	6.06
4	2.20 ± 0.02	3.06	1.280 ± 0.009	4.04
5	2.16 ± 0.12	1.56	1.272 ± 0.005	3.43

TABLE I. Results for Method 1 (averages using Bragg's Law) of the experiment in average atomic plane spacing for the outer diffraction ring ($\overline{d_{10}}$) and the inner diffraction ring ($\overline{d_{11}}$), as well as the percent error for each ($\delta_{d_{10}}$ and $\delta_{d_{11}}$ respectively). Trial 2 is the pseudo-random run order sequence, where voltages to the anode were chosen non-sequentially (this is not strictly random). Note the difference in uncertainties with this trial from the others. The theoretical values are $d_{11} = 2.13$ Å and $d_{10} = 1.23$ Å.

If we check the ratio of these spacings, they should be $\frac{d_{11}}{d_{10}} \approx \sqrt{3}$. Selecting the result from trial 5 as the representative result: $\frac{2.16}{1.23} = 1.698$, which expressed as a ratio over the accepted value should be very near 1: $\frac{1.698}{1.732} = 0.98$. This result is promising.

These results are strong indicators for the validity of Bragg's Law. Collecting the data R_{in}, R_{out} for various V allows a direct tabulation of d. This method is compelling since the result d_{11} agrees with theoretical predictions using only the geometry of the crystal structure (see Fig 2) and the values given by the manufacture. The values for d_{10} are near the accepted values.

4.2 Method 2: Slope of Best-Fit

Method 2 analyzes the same data by finding the best-fit slope m of the diffraction ring diameter vs. the inverse square voltage (the function is Eq 6). The slopes of these plots are used to find d for the inner and outer rings, by the relation $d = \frac{2L}{m}\sqrt{150}$. Since choosing the x-axis to be the inverse square voltage generates a linear trend in the data points, the SciPy curve_fit() routine returns parameters for the y-intercept and slope of a line. Visual inspection of the generated plots (Fig 6) shows such a trend.

Trial	d_{11} (Å)	$\delta_{d_{11}}$ (%)	d_{10} (Å)	$\delta_{d_{10}}$ (%)
1	1.81 ± 0.06	14.80	1.27 ± 0.09	3.51
2	2.8 ± 0.3	29.73	1.33 ± 0.12	8.11
3	1.84 ± 0.09	13.41	1.32 ± 0.14	7.29
4	2.01 ± 0.15	5.48	1.19 ± 0.08	2.44
5	2.01 ± 0.09	5.56	1.20 ± 0.04	2.38

TABLE II. Results for Method 2 (using slope of best fit) of the experiment in average atomic plane spacing for the outer diffraction ring ($\overline{d_{10}}$) and the inner diffraction ring ($\overline{d_{11}}$), as well as the percent error for each ($\delta_{d_{10}}$ and $\delta_{d_{11}}$ respectively). Again, trial 2 is the pseudo-random trial. The theoretical values are $d_{11} = 2.13$ Å and $d_{10} = 1.23$ Å.

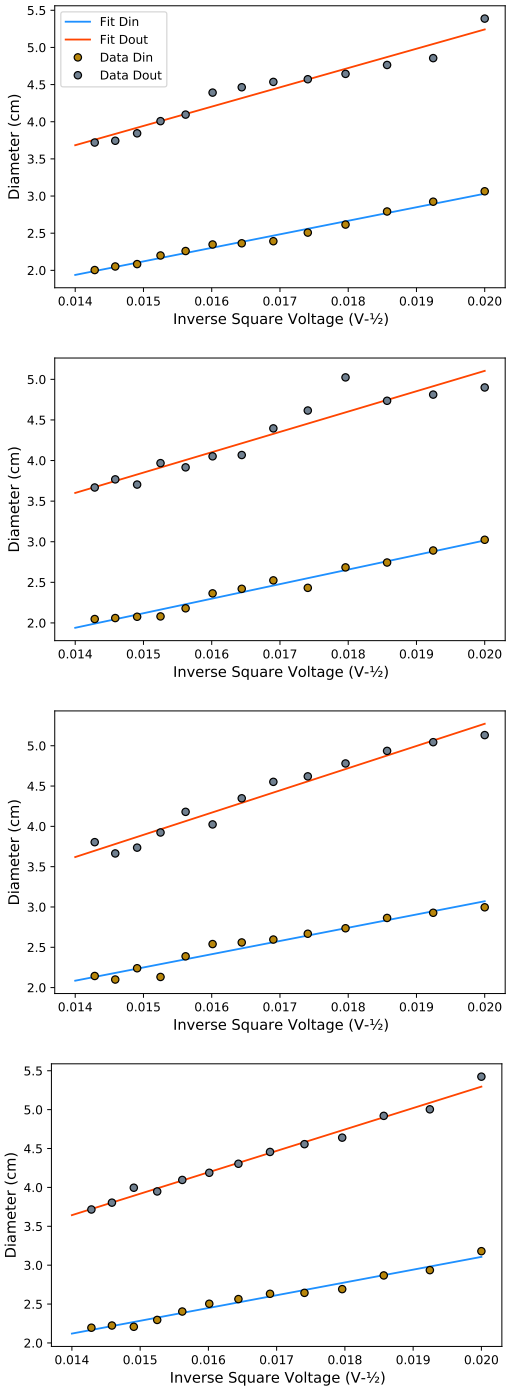

Figure 6. The data for the four non-random trials. The trials are in order from top to bottom: trial 1, trial 3, trial 4, and trial 5. The diameter of the diffraction rings are plotted as a function of the inverse-square voltage. Each sub-graph contains the best-fit line and the plot of the data for both the inner and outer diffraction rings (see legend in the first graph. The color scheme is consistent across all graphs.).

Trial 5 has the best agreement with the theoretical predictions for both d_{11} and d_{10}. Again, finding the ratio of the reflection plane spacings should be $\sqrt{3}$. Checking, $\frac{2.01}{1.20} = 1.675$. If this value is accurate, then the ratio of it with the accepted $\sqrt{3}$ should be very near 1: $\frac{1.675}{1.732} = 0.967$. This result is also promising - the results agree with the dimensionless ratio derived from geometric fact, if $\gamma = 120^\circ$ and $a = b = 2.46$ Å are assumed to be true. However, there is still one glaring issue for both method 1 and method 2: bias in the measurement process.

Notice the uncertainties associated with trial 2. As mentioned in Sec 3, this trial is the 'random' sample sequence trial. Again, the run ordering of this trial were not strictly random - the ordering sequence should come from a random number generator, and if the experiment were to be performed again, certainly that would be the run order selection process. Instead, the sequence ordering was selected on a whim by the experimenter. There is an argument to be made that this is not strictly random (that is why trial 2 has been identified as the 'pseudo-random' trial - randomness was the goal but from rigorous perspective it was not random at all).

While the trial 2 data may not have been collected in a truly random process, there are some features of the data that distinguish it from the other trials. In the graph for trial 2 (Fig 7), there is a noticeable difference in the residual deviation from the mean and those from the other trials (see Fig 6). Further, each sequential data point does not follow any trend; they sporadically appear above or below the mean. A range of the data in Trial 3 in Fig 6 (from about $0.017\text{V}^{-1/2}$ to $0.0185\text{V}^{-1/2}$) shows some comparable levels of variance to the second trial, but the variance follows a trend (roughly, a line), and trials 1, 4, and 5 show very little variance from the mean (best fit lines).

The statistical features of trial 2 are likely the result of bias. This is because the data collected for them were selected preferentially based on the bias of the experimenter. During the collection of data, each reading would be compared to previous readings to ensure that it was 'on track', i.e. that the response (diameter) was in line with what would be expected for a specific change of the control (voltage). For increasing voltages, the reading was checked to see that the diameter was sufficiently *less* than the previous reading (where 'sufficient' is defined by the expected, regular interval between previous diameter readings). At times, this would result in re-taking the measurement. This also explains the lower uncertainties. Since this was the only controlled difference between the trial 2 and the others, it would seem that this process contributed significantly to the trend in the data, and therefore to the uncertainties in the results obtained from the data. The uncertainties are included in Table I.

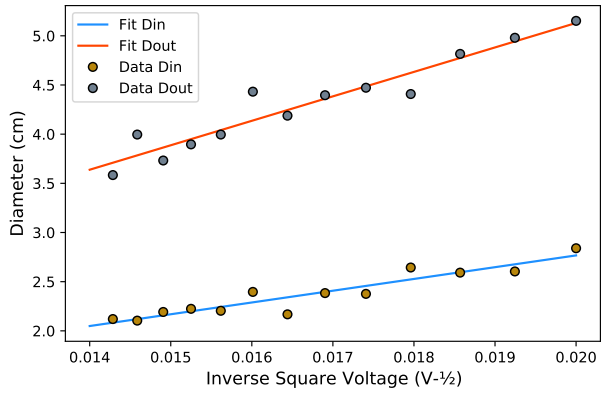

Figure 7. The plot of the best fit line against data collected in the psuedo-random measurement run order trial (second trial).

If data is collected over time with increasing or decreasing predictor variables (such as the voltage)), then it becomes difficult to separate drift from the functional response being tested[4]. Trial 2 was intended to explore the relationship between a randomised process against a non-randomized one. It would seem that, more than anything, it highlighted bias on the part of the experimenter for trials 1, 3, 4 and 5. The pseudo-random trial 2 eliminated the bias, since subsequent measurements could not be readily checked to agree with the current measurement. Such selection bias should be avoided. The idea is to test the theory. If measurements are being selected with preference for the theory, then it is not a valid test, and in-fact is opposed to the core tenets of the scientific method. If the experiment were performed again.

Due to the bias issues, only the results from the pseudo-random trial 2 ought to be considered for the qualitative results of the experiment. For method 1, we have $\frac{2.4}{1.31} = 1.832$, and for method 2 we have $\frac{2.8}{1.33} = 2.105$ These ratios are still close to the accepted ratio, $\sqrt{3} \approx 1.732$, but the results are not as close to the accepted value as they are with the other, biased trials, as was already discussed.

5 Conclusion

The wave-nature of matter as predicted by Louis de Broglie was verified, and topics relating to the interaction of subatomic particles and solid state crystal structures were examined, namely diffraction patterns and plane reflection geometries for electron beams of various wavelengths incident on graphite sample. More specifically, two diffraction rings were produced, and by two different methods, the distance between sequential planes of reflection for each maxima d_{11} and d_{10} were deduced from the data collected. The results agree with geometric analysis of the crystal structure of graphite - albeit, with a glaring issue in the measurement process resulting from experimenter bias. In order to eliminate the possibility of bias and to help reduce possible systematic error in the form of drift, the experiment should be performed again, with the run-sequence of the data collection process taken in truly random order. This could be done by assigning a number to each value of the control (voltages in the range $2.5\,\mathrm{kV}$ to $4.9\,\mathrm{kV}$) and then using a random number generator to select the voltage for each measurement.

[4]NIST, "NIST/SEMATECH e-Handbook of Statistical Methods"

References

[1] Krane, Kenneth S. Modern Physics. Wiley, 2020. .

[2] Gray, Dodd, et al. “Crystal Structure of Graphite, Graphene and Silicon.” Graphene.pdf, WVU, 13 Mar. 2009, community.wvu.edu/ miholcomb/graphene.pdf.

[3] Instruction Manual: Electron Diffraction Tube - Welch Scientific Co. Cat. No. 2639

[4] NIST/SEMATECH e-Handbook of Statistical Methods, http://www.itl.nist.gov/div898/handbook/, 4/11/2021)